Journal of Inorganic and General Chemistry

ZAAC

Zeitschrift für anorganische und allgemeine Chemie

**Title:** Synthesis, Crystal and Electronic Structure of La2SiP4

**Authors:** Georgiy Akopov, Gayatri Viswanathan, and Kirill Kovnir

**To be cited as:** *Z. anorg. allg. Chem.* 10.1002/zaac.202000378

**Link to VoR:** https://doi.org/10.1002/zaac.202000378

WILEY-VCH

www.zaac.wiley-vch.de

10.1002/zaac.202000378

# Synthesis, Crystal and Electronic Structure of $La_2SiP_4$

Georgiy Akopov[1,2], Gayatri Viswanathan[1,2], Kirill Kovnir[1,2,*]

[1]*Ames Laboratory, U.S. Department of Energy, Ames, IA 50011, United States;*

[2]*Department of Chemistry, Iowa State University, Ames, IA 50011, United States.*

*Corresponding authors: kovnir@iastate.edu

*Dedicated to Professor Sven Lidin on the Occasion of his 60th Birthday.*

## ABSTRACT

$La_2SiP_4$ (*mP*-28, $Z = 4$, Wyckoff sequence $e^7$, space group $P2_1/c$ (No. 14), $a = 10.8230(6)$ Å, $b = 7.5208(4)$ Å, $c = 7.9189(4)$ Å, and $\beta = 105.389(2)^o$) which crystallizes in the $La_2CuS_4$ structure type is reported. Instead of isolated $CuS_3$ triangles bridged by disulfide anions, in the crystal structure of $La_2SiP_4$, one-dimensional zig-zag chains composed of $SiP_4$ tetrahedra connected by P-P bonds are present. Lanthanum cations fill the voids between the chains and are coordinated by either 9P or 8P+Si atoms. DFT calculations predict $La_2SiP_4$ to be a narrow bandgap semiconductor with $E_g = 0.35$ eV.

## INTRODUCTION

Metal tetrel-pnictides (*ATtPn*, *A* = electropositive metal, *Tt* = Si, Ge and Sn, *Pn* = P and As) are a large family of compounds showing a variety of crystal structures and atom connectivity and exhibiting exciting transport, magnetic, and optical (NLO) properties.[1–9] The underlying *Tt*-*Pn* anionic sublattice can range from isolated $TtPn_4$ tetrahedra ($Ca_4SiP_4$, $Sr_4SiP_4$, $Ba_4SiP_4$, $Li_8SiP_4$ and $Li_8GeP_4$), 1D-chains ($Ca_3Si_2P_4$ and $K_2SiP_2$), 2D-layers ($LiGe_3P_3$, $LiGe_3As_3$, $Cs_{0.16}SiAs_2$, $Ca_2Si_2P_4$, $Li_{1-x}Sn_2As_2$), to 3D-frameworks ($Li_2GeP_2$, $SrSi_7P_{10}$, $BaSi_7P_{10}$, $Li_2SiP_2$, $LiSi_3As_6$, $MgSiAs_2$, $Mg_3Si_6As_8$, and $Ca_3Si_8P_{14}$).[2,7,10–24] The tetrel-pnictide tetrahedral unit can be connected to its neighbors via sharing vertices and edges, or by P-P bonds.[1,13,25–27]

Among metal tetrel-pnictides, $AE_2SiP_4$ (*AE* = Sr, Eu, and Ba) is an interesting class of compounds.[27–29] Sr- and Eu-containing 2-1-4 compounds are isostructural to tetragonal-$Ba_2SiP_4$ and are characterized by $SiP_4$ units connected to each other via P-P bonds forming a polar 3D-network.[29] Orthorhombic-$Ba_2SiP_4$ on the other hand has $SiP_4$ tetrahedra connected by P-P bonds forming 1D-chains.[28]

Here we report the newest member of the 2-1-4 family, $La_2SiP_4$, crystallizing in the monoclinic $P2_1/c$ space group. This structure is related to the ternary sulfide, $La_2CuS_4$;[30] however unlike the latter, which has isolated $CuS_3$ triangles bridged by disulfide ions, the phosphide has $SiP_4$ tetrahedra connected via P-P bonds forming 1D zig-zag chains along the [001] direction.

## RESULTS AND DISCUSSION

A single crystal of $La_2SiP_4$ was serendipitously extracted from a sample with a nominal composition of $LaSiP_3$. $La_2SiP_4$ crystallizes in the monoclinic $P2_1/c$ (no. 14) space group, Pearson symbol *mP*-28, $Z = 4$, Wyckoff sequence $e^7$, with the lattice parameters $a = 10.8230(6)$ Å, $b =$

7.5208(4) Å, $c$ = 7.9189(4) Å, and $\beta$ = 105.389(2)° (**Figure 1** and **Table 1**). After the determination of the structure and composition, a bulk sample of $La_2SiP_4$ was synthesized using a pre-arc-melted lanthanum silicide precursor with nominal composition $La_2Si$, and a stoichiometric amount of phosphorus, as a dark-grey polycrystalline powder (see **Experimental Section**). The main phases present in the PXRD spectrum are $La_2SiP_4$ and LaP, with minor admixtures being SiP and $LaP_2$. The presence of LaP can be explained by the fact that the precursor with the nominal composition of 2La:Si, contains $La_5Si_3$ phase as well as La metal, which upon reaction with P produces LaP. Attempts to synthesize the $La_2SiP_4$ from the stoichiometric mixture of elements resulted in the formation of binary phosphides. The as-synthesized samples of $La_2SiP_4$ were stable in air for at least an hour, however samples stored in air for several days changed color and $La_2SiP_4$ decomposed into mixture of $La_2Si_2O_7$ and amorphous phases according to X-ray powder diffraction. The presence of admixtures in the samples and low tolerance of $La_2SiP_4$ towards moisture and/or air prevented properties characterization.

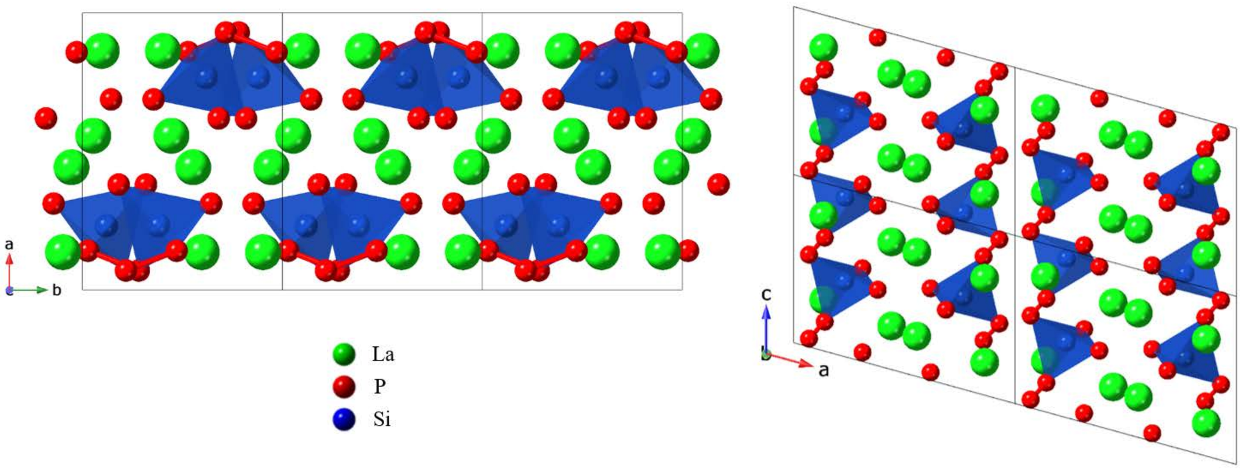

**Figure 1.** Crystal structure of $La_2SiP_4$. $SiP_4$ tetrahedra are connected via P – P bonds to each other forming zig-zag chains propagating along the $c$-axis. La - green; Si (atoms and tetrahedra) - blue; P – red.

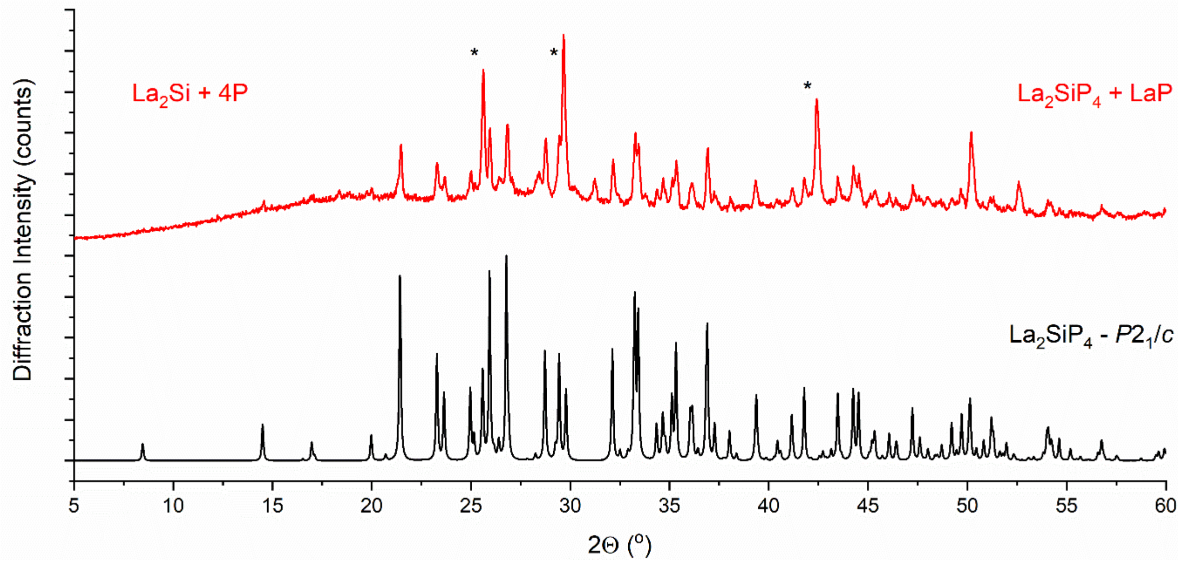

**Figure 2.** PXRD patterns for $La_2SiP_4$ sample synthesized by annealing at 1000 °C and a dwell time of 192 hours. Pattern in black is calculated from the single crystal structural model; pattern in red is experimental. (*) denotes diffraction peaks corresponding to LaP, additional lower intensity impurity peaks correspond to SiP and $LaP_2$.

**Table 1.** Crystallographic data of $La_2SiP_4$.

| | **$La_2SiP_4$** |
|---|---|
| **CSD-number** | 2036741 |
| **Space group** | $P2_1/c$ (no.14) |
| **$\lambda$ (Å)** | Mo-$K\alpha$: 0.71073 |
| **$T$ (K)** | 100(2) |
| **$a$ (Å)** | 10.8230(6) |
| **$b$ (Å)** | 7.5208(4) |
| **$c$ (Å)** | 7.9189(4) |
| **$\beta$ (°)** | 105.389(2) |
| **$V$ (Å$^{-3}$)** | 621.47(6) |
| **$Z$** | 4 |
| **$\rho$ (g•cm$^{-3}$)** | 4.59 |
| **$\mu$ (mm$^{-1}$)** | 14.64 |
| **$\theta$ (°)** | 3.34 < θ < 25.24 |
| **Data / param.** | 5093/64 |
| **$R_1$** | 0.019 |
| **$wR_2$** | 0.033 |
| **Goodness-of-fit** | 1.104 |
| **Diff. peak/hole (e•Å$^{-3}$)** | 1.67/-1.66 |

*All atomic sites have 100% occupancy*

| **Atom** | **Wyckoff position** | ***x/a*** | ***y/b*** | ***z/c*** | $U_{eq}$/Å$^2$ |
|---|---|---|---|---|---|
| La1 | 4*e* | 0.4432(2) | 0.9456(2) | 0.7598(2) | 0.00306(1) |
| La2 | 4*e* | 0.1368(3) | 0.9031(2) | 0.3043(2) | 0.00464(2) |
| P1 | 4*e* | 0.3120(3) | 0.6437(5) | 0.5550(5) | 0.00401(5) |
| P2 | 4*e* | 0.3807(3) | 0.1817(5) | 0.4526(5) | 0.00445(5) |
| P3 | 4*e* | 0.0705(3) | 0.2822(5) | 0.5493(5) | 0.00491(5) |
| P4 | 4*e* | 0.1417(3) | 0.0285(5) | 0.6759(5) | 0.00441(5) |
| Si1 | 4*e* | 0.2322(4) | 0.3806(5) | 0.4491(5) | 0.00379(6) |

$La_2SiP_4$ crystallizes in the $La_2CuS_4$ structure type,[30] however, unlike Cu in the sulfide, Si atoms in the crystal structure of $La_2SiP_4$ are tetrahedrally coordinated with four P atoms. The distances in $SiP_4$ tetrahedra vary in the 2.191 - 2.232 Å range, which is in good agreement with other ternary metal silicon phosphides.[12,21,31–33] Each $SiP_4$ tetrahedron is connected to two other tetrahedra via homonuclear P-P bonds to form one dimensional zig-zag chains (**Figure 1**) propagating along [001] direction. The P-P bond length of 2.198 Å is typical for single P-P bond found in other metal phosphides.[34–37] Lanthanum atoms are located between the $SiP_4$ chains. Both $La^{3+}$ cations are coordinated by nine atoms, either 8P+Si (La1) or 9P (La2) with *d*(La-P/Si) = 2.929-3.40 Å (**Figure 3**). Similar La-P distances are found in La-{Cu,Zn}-P complex phosphides: $LaCu_4P_3$[38], $LaCu_{1+x}P_2$[38], $La_{1.6}Ba_{6.4}Cu_{16}P_{30}$[39], $La_2Zn_{11}P_9$, and $La_4Zn_7P_{10}$[40,41]. La@$P_9$ and La@$SiP_8$ polyhedra share corners, edges, and faces.

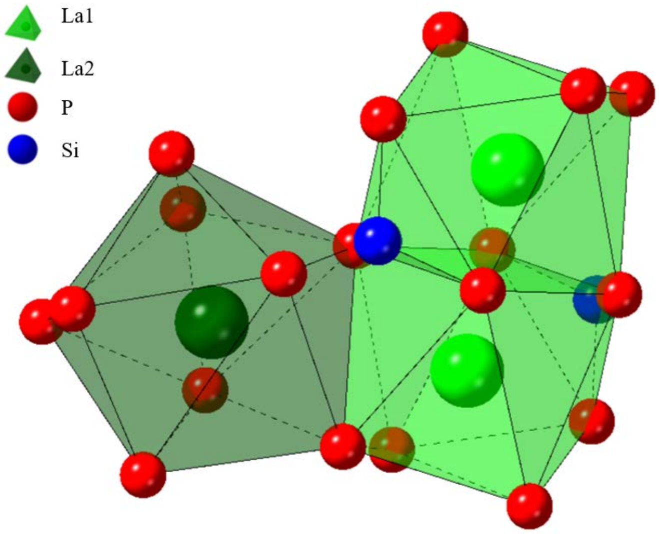

**Figure 3.** Coordination of the lanthanum atoms (green) in the crystal structure of $La_2SiP_4$: La1 is coordinated by 8P+1Si, while La2 is coordinated by 9P atoms.

The $La_2SiP_4$ crystal structure is related to the structure of $La_2CuS_4$ ternary metal sulfide (**Figure 4**).[30] $La_2CuS_4$ crystallizes in the same space group ($P2_1/c$), but is characterized by discrete anion triplets $[S_3Cu\text{--}S\text{—}S\text{--}CuS_3]^{12-}$, where slightly out-of-plane $[CuS_3]^{5-}$ triangles are bridged by disulfide anions $[S_2]^{2-}$. $La^{3+}$ cations are surrounded by bicapped trigonal prims of sulfur.

Further structural similarities can be found with $Ba_2SiP_4$ (**Figure 4**).[27–29] In the crystal structure of the orthorhombic polymorph (space group *Pnma*), $Ba^{2+}$ atoms are located in-between the $SiP_4$ chains but are capped by three different types of polyhedra: elongated square pyramids, cubes, and elongated square bipyramids. Although the composition is the same, due to a different charge on the cation: $Ba^{2+}$ vs $La^{3+}$, the resulting connectivity of $SiP_4$ tetrahedra is different. In $Ba_2SiP_4$, $SiP_4$ tetrahedra are linked by P-P bonds (d(P-P) = 2.23 Å)[28] forming chains along the *b*-direction. In the crystal structure of $Ba_2SiP_4$ every $SiP_4$ tetrahedron is engaged in four P-P bonds, i.e. all the P vertices participate in P-P bonding. The same is true for tetragonal $Ba_2SiP_4$ (space group $I\bar{4}2d$)

where all vertices of $SiP_4$ tetrahedra form P-P bonds resulting in 3D framework.[27,29] Increasing of the cation charge leads to the reduction of P atoms and in the crystal structure of $La_2SiP_4$ only two tetrahedral vertices form P-P bonds.

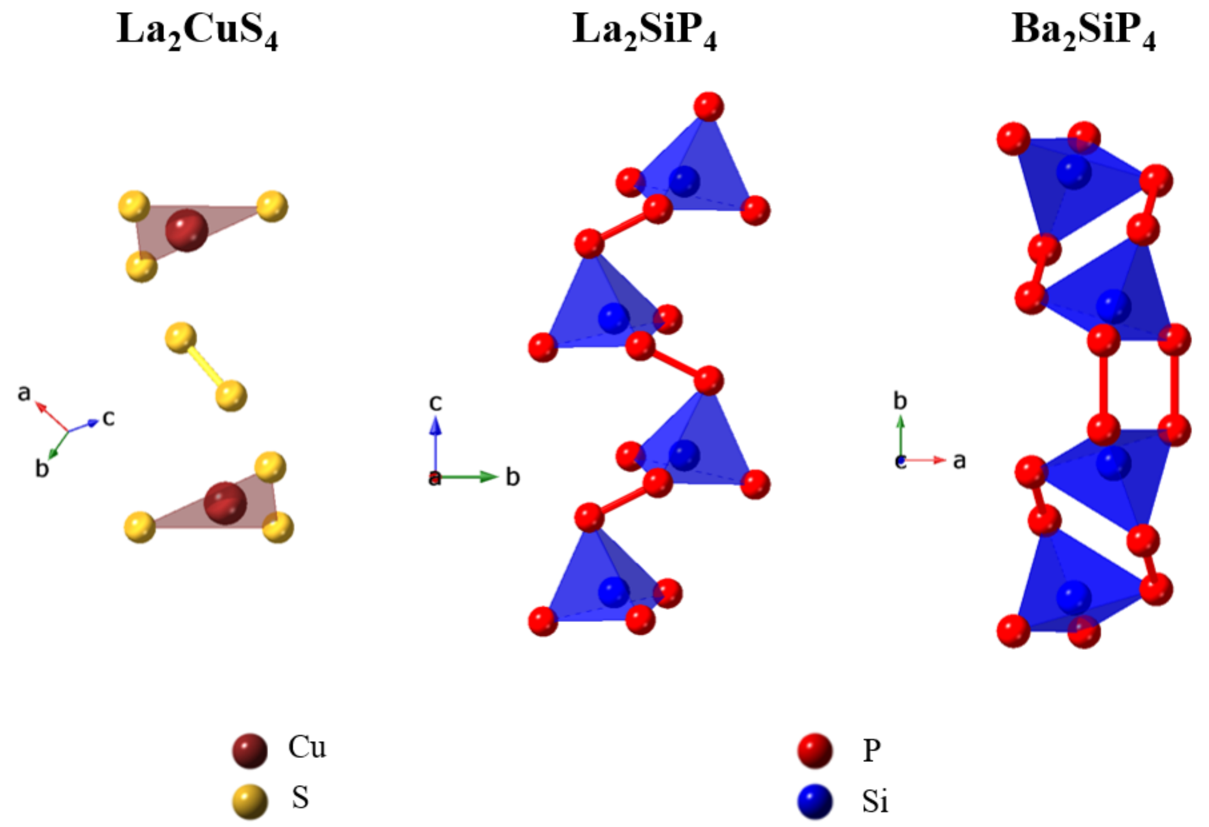

**Figure 4.** Comparison of the connectivity for the $CuS_4$ and $SiP_4$ units in $La_2CuS_4$ (**left**), $La_2SiP_4$ (**middle**), and *o*-$Ba_2SiP_4$ (**right**). For $La_2CuS_4$, slightly-out-of-plane $[CuS_3]^{5-}$ units are bridged by $[S_2]^{2-}$ anions. For $La_2SiP_4$, $[SiP_4]^{-}$ tetrahedra are linked by two P-P bonds forming zig-zag chains along *c*-axis. For $Ba_2SiP_4$, $[SiP_4]$ tetrahedra are linked via four P-P bonds forming zig-zag chains along *b*-axis.

Upon crystal structure determination, it is difficult to distinguish P and Si due to similarity of their scattering factors. Initial atomic site assignment was made based on local coordination assuming Si is surrounded by 4P. After that the occupancy of each site set as either Si or P was independently refined. The occupancy of Si1 site when refined as P was 0.958(2), while refined as Si it was 0.999(2). Similarly, the P sites occupancy when refined as P were 0.993(2)-0.996(2) while refinement of those sites as Si clearly resulted in occupancies exceeding 100%, i.e. 1.036(2)-1.041(2). The final refinement ADPs (atomic displacement parameters) were similar for the proposed Si and P sites indicating the correctness of the structural model (Table 1 and Figure 5). Elemental composition was confirmed using Energy Dispersive Spectroscopy at Scanning Electron Microscope which show the average composition of the compound to be $La_2Si_{1.5(1)}P_{4.2(1)}$. Note that the overestimation of the light elements content is common for this method.

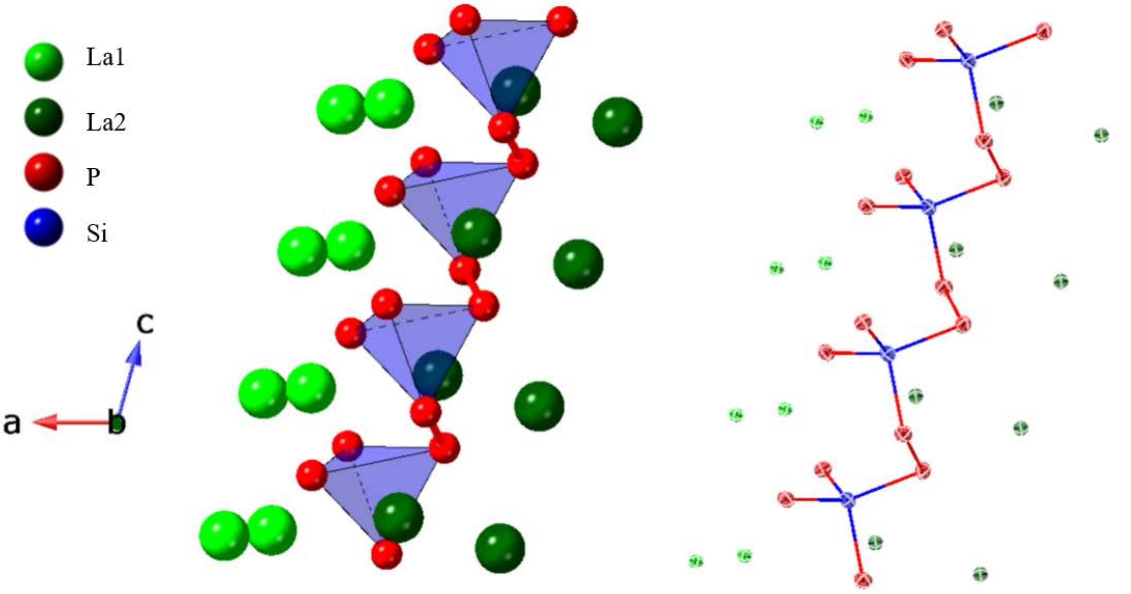

**Figure 5.** (**Left**) polyhedral view of $SiP_4$ chains in $La_2SiP_4$ along the [001] direction; (**right**) a similar view plotted with displacement ellipsoids (99% probability).

The number of P-P bonds in $La_2SiP_4$ and $Ba_2SiP_4$ can be explained by electron counting and charge balance. In $Ba_2SiP_4$, assuming +4 formal charge of Si, the electron balanced formula can be written as $(Ba^{2+})_2(Si^{4+})(P^{2-})_4$, implying that every P atom should form one P-P bond. In $La_2SiP_4$, the metal cation is $La^{3+}$, making the formal electron count $(La^{3+})_2(Si^{4+})(P^{2-})_2(P^{3-})_2$, implying that only half P atoms should be engaged in P-P bonding.

The electronic structure of $La_2SiP_4$ was calculated using the Vienna ab initio simulation package (VASP). The crystal structure was treated in triclinic *P*1 symmetry and allowed to relax freely allowing for optimization of atomic positions as well as unit cell size and shape. The symmetry of the resulting unit cell was evaluated using FINDSYM in the ISOTROPY software suite.[42,43] The DFT-optimized lattice parameters ($a$ = 10.6790 Å, $b$ = 7.3716 Å, $c$ = 7.7654 Å, $\beta$ = 105.0304º) and atomic positions agree reasonably with the experimentally determined crystal structure. The optimized, relaxed structure was used for density of states (DOS) calculations which revealed that $La_2SiP_4$ is a narrow bandgap semiconductor with a calculated bandgap of 0.35 eV (**Figure 6**). Near the Fermi level, the primary contribution to the DOS in the valence band is from P states with substantial contribution from La and small contribution from Si. In the conduction band, La states dominate with minor contributions from Si and P. Similar mixing of P and La states in the top of valence band was calculated for $La_2Ba_6Cu_{16}P_{30}$[39] which was shown to have significant impact on charge transport properties of that clathrate material. Unfortunately, the experimental studies of the properties of $La_2SiP_4$ were hampered by presence of LaP admixture and high sensitivity of $La_2SiP_4$ towards moisture and air.

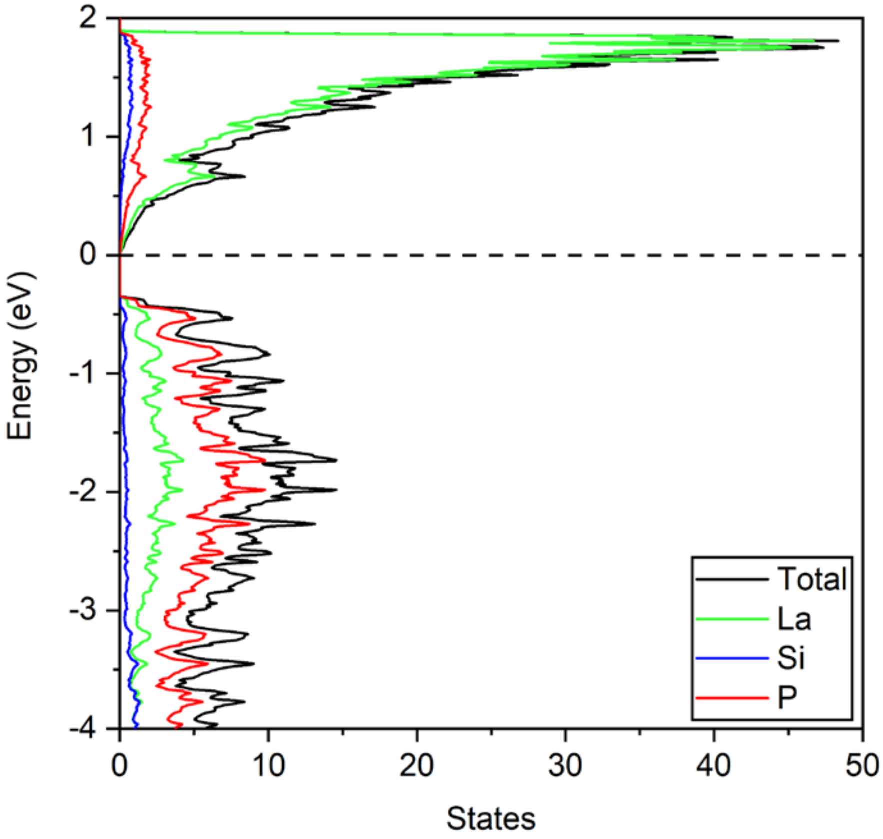

**Figure 6.** Total and partial DOS for $La_2SiP_4$. $La_2SiP_4$ is a narrow bandgap semiconductor with a calculated bandgap of 0.35 eV.

## CONCLUSIONS

$La_2SiP_4$ is the newest member of the $M_2SiP_4$ family, related to the $La_2CuS_4$ ternary sulfide. In the crystal structure of $La_2SiP_4$ the $SiP_4$ tetrahedra are connected to their neighbors by P-P bonds forming zig-zag chains along the [001] direction. $La^{3+}$ cations occupy the voids between the chains and are coordinated by either 9 P or 8P+1Si atoms. According to band structure calculations, $La_2SiP_4$ is predicted to be a semiconductor with a 0.35 eV band gap.

## EXPERIMENTAL METHODS

### Synthesis

Si chips (99.9999%, Strem, USA), red P powder (98.9%, Alfa Aesar, USA), La ingots (99.9999%, Ames Lab, USA) were used as received. Lanthanum was acquired from the Materials Preparation Center at Ames Laboratory, which is supported by the US DOE Basic Energy Sciences.

Synthesis of $La_2SiP_4$ was done using pre-arc-melted precursors. The La-Si precursors were prepared using cut La pieces and Si chips (**Figure 7**). The samples with a total mass of 0.5 g were weighed out in a ratio of La:Si = 2:1.05 to account for the evaporation of silicon. The samples were then placed in the arc-melter onto a Cu hearth (Zr metal was used as oxygen getter material). The arc-melter chamber was later sealed and evacuated for 20 minutes followed by purging with Ar, this process was repeated 2-3 times to ensure that no oxygen was present in the chamber. During arc-melting, the getters were melted first to ensure the absorbance of any trace oxygen, and then the samples were heated for ~1 minute at a current of $I \sim 70$ Amperes (A) until molten, then allowed to solidify, flipped and re-arced 2 more times to ensure homogeneity under a current of $I \sim 100$ A. The precursor ingots were then crushed into a powder using a tool steel Plattner-style diamond crusher.

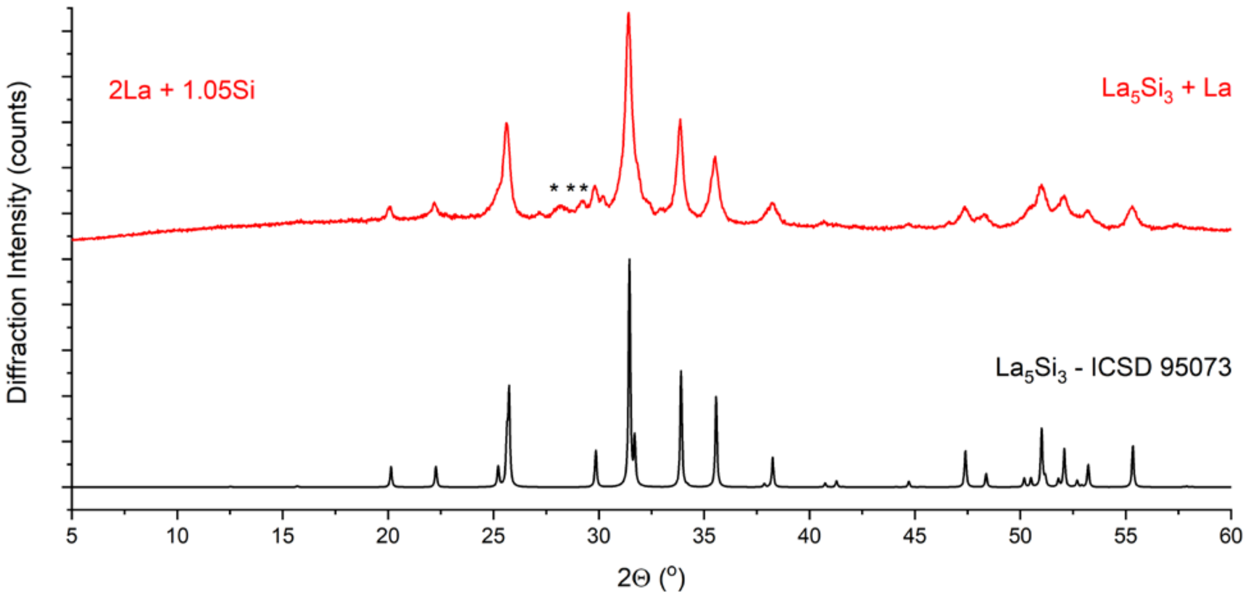

**Figure 7.** PXRD pattern showing phase formation for the arc-melted precursor with a nominal composition of $La_2Si_{1.05}$. Pattern in black is calculated pattern for $La_5Si_3$; pattern in red is experimental. (*) denotes peaks corresponding to La metal.

Single crystals of $La_2SiP_4$ ($P2_1/c$) were serendipitously extracted from products of the annealing of sample composed from LaSi precursor and 3 times molar excess of P.

***HAZARD:** The amount of P in reaction should be kept at a minimum because, due to relatively high temperatures of synthesis, the vapor pressure of P produced may be sufficient to cause the sealed ampoule to shatter or explode!*

After the single crystal XRD determination of crystal structure and composition of a new ternary metal phosphide, $La_2SiP_4$, several attempts were made to synthesize this phase as bulk powder. This was done using pre-arc-melted (2La:Si) precursor and stoichiometric amount of phosphorus. Samples were prepared by loading the silicide binary and phosphorus into a silica ampoule in a 1:4 precursor to phosphorus molar ratio, respectively. The ampoule was then flame sealed under vacuum. Several attempts were made with variable temperature and dwell times. It was found that the best results for $La_2SiP_4$ phase were for an annealing at 1000 $^{o}$C (14 hours heating and 10 hours cooling) with a dwell time of 192 hours. Using this profile, the percent yield of the title compound

10.1002/zaac.202000378

is 85% (average of two samples) by profile refinement method. Attempts to make a Ce and Gd analogues of $La_2SiP_4$ and their solid solution (e.g. $LaCeSiP_4$) were not successful. $La_2SiP_4$ possesses limited stability in ambient atmosphere (moisture and air) and over time decomposes into $La_2Si_2O_7$ and amorphous products.

### X-ray Diffraction

Powder X-ray diffraction (PXRD) was performed using a Rigaku Miniflex 600 with Cu-$K_\alpha$ radiation and a Ni-$K_\beta$ filter. Sample holders were composed of a zero-background silicon plates.

Single crystal X-ray diffraction (SCXRD) was performed using a Bruker D8 Venture diffractometer using Mo-$K_\alpha$ radiation. The datasets were collected at 100 K under a $N_2$ stream with ω-scans recorded at a 0.3° step width and integrated with the Bruker SAINT software package. Structure determination and refinement of the crystal structures were carried out using the SHELX suite of programs.[44]

### Scanning Electron Microscopy/Energy Dispersive Spectroscopy (SEM/EDS)

Elemental analysis was conducted using a FEI Quanta 250 field emission-SEM with EDS detector (Oxford X-Max 80, ThermoFischer Scientific, Inc., USA) and Aztec software. Powder samples were mounted on carbon tape. The energy of the electron beam used was held constant at 15 kV and a working distance of 10.5 mm was used.

### Electronic Structure Calculations

First principles calculations were performed on $La_2SiP_4$ using the Vienna ab initio simulation package (VASP), which uses a plane-wave basis set with projector-augmented-wave (PAW) potentials.[45–47] Perdew-Burke-Ernzerhof (PBE) generalized gradient functionals were employed with an energy cutoff of 500 eV.[48,49] A *Γ*-centered Monkhorst-Pack *k*-point grid of 10×14×14 was employed for integrating the irreducible wedge of the first Brillouin zone by the linear tetrahedron method.[50,51] Electronic and structure optimization criteria were set to $1\times10^{-4}$ eV and -0.02 eV, respectively.

## ACKNOWLEDGEMENTS

We would like to thank Prof. Vitalij Pecharsky (Iowa State University and Ames Laboratory) for the access to the arc-melting setup. G.A. gratefully acknowledges financial support from the Ames Laboratory Spedding Postdoctoral Fellowship. This work was supported by the Ames Laboratory's Laboratory Directed Research and Development (LDRD) program. The Ames Laboratory is operated for the U.S. DOE by Iowa State University under contract # DE-AC02-07CH11358.

## KEYWORDS

Lanthanum; silicon; phosphorus; crystal structure; chemical bonding; tetrahedra; chains.

## ORCID

| | |
|---|---|
| Georgiy Akopov | 0000-0001-9399-9850 |
| Gayatri Viswanathan | 0000-0002-9693-8225 |
| Kirill A. Kovnir | 0000-0003-1152-1912 |

## REFERENCES

[1] A. J. Springthorpe, J. G. Harrison, *Nature* **1969**, *222*, 977–977.

[2] K. E. Woo, J. Wang, K. Wu, K. Lee, J.-A. Dolyniuk, S. Pan, K. Kovnir, *Adv. Funct. Mater.* **2018**, *28*, 1801589.

[3] B. Kocak, Y. O. Ciftci, G. Surucu, *Journal of Elec Materi* **2017**, *46*, 247–264.

[4] S. Cheddadi, H. Meradji, S. Ghemid, L. Tairi, S. B. Omran, R. Khenata, *Physica B: Condensed Matter* **2018**, *530*, 24–29.

[5] V. L. Shaposhnikov, A. V. Krivosheeva, V. E. Borisenko, J.-L. Lazzari, F. A. d'Avitaya, *Phys. Rev. B* **2012**, *85*, 205201.

[6] H. Pfister, *Acta Cryst* **1958**, *11*, 221–224.

[7] K. Lee, D. Kaseman, S. Sen, I. Hung, Z. Gan, B. Gerke, R. Pöttgen, M. Feygenson, J. Neuefeind, O. I. Lebedev, K. Kovnir, *J. Am. Chem. Soc.* **2015**, *137*, 3622–3630.

[8] Y. Goto, A. Miura, C. Moriyoshi, Y. Kuroiwa, T. D. Matsuda, Y. Aoki, Y. Mizuguchi, *Sci Rep* **2018**, *8*, 12852.

[9] Y. Goto, A. Yamada, T. D. Matsuda, Y. Aoki, Y. Mizuguchi, *J. Phys. Soc. Jpn.* **2017**, *86*, 123701.

[10] A. Haffner, T. Bräuniger, D. Johrendt, *Angew. Chem. Int. Ed.* **2016**, *55*, 13585–13588.

[11] B. Eisenmann, H. Jordan, H. Schäfer, *Materials Research Bulletin* **1982**, *17*, 95–99.

[12] B. Eisenmann, H. Jordan, H. Schäfer, *Zeitschrift für Naturforschung B* **1984**, *39*, 864–867.

[13] X. Zhang, T. Yu, C. Li, S. Wang, X. Tao, *Z. anorg. allg. Chem.* **2015**, *641*, 1545–1549.

[14] J. Mark, M. P. Hanrahan, K. E. Woo, S. Lee, A. J. Rossini, K. Kovnir, *Chem. Eur. J.* **2019**, *25*, 6392–6401.

[15] K. E. Woo, J.-A. Dolyniuk, K. Kovnir, *Inorg. Chem.* **2019**, *58*, 4997–5005.

[16] J. Mark, K. Lee, M. A. T. Marple, S. Lee, S. Sen, K. Kovnir, *J. Mater. Chem. A* **2020**, *8*, 3322–3332.

[17] H. Eickhoff, L. Toffoletti, W. Klein, G. Raudaschl-Sieber, T. F. Fässler, *Inorg. Chem.* **2017**, *56*, 6688–6694.

[18] T. F. Fässler, H. Eickhoff, V. Hlukhyy, *Z. anorg. allg. Chem.* **2020**, zaac.202000316.

[19] S. Strangmüller, H. Eickhoff, G. Raudaschl-Sieber, H. Kirchhain, C. Sedlmeier, L. van Wüllen, H. A. Gasteiger, T. F. Fässler, *Chem. Mater.* **2020**, *32*, 6925–6934.

[20] S. Strangmüller, H. Eickhoff, D. Müller, W. Klein, G. Raudaschl-Sieber, H. Kirchhain, C. Sedlmeier, V. Baran, A. Senyshyn, V. L. Deringer, L. van Wüllen, H. A. Gasteiger, T. F. Fässler, *J. Am. Chem. Soc.* **2019**, *141*, 14200–14209.

[21] L. Toffoletti, H. Kirchhain, J. Landesfeind, W. Klein, L. van Wüllen, H. A. Gasteiger, T. F. Fässler, *Chem. Eur. J.* **2016**, *22*, 17635–17645.

[22] H. Eickhoff, S. Strangmüller, W. Klein, H. Kirchhain, C. Dietrich, W. G. Zeier, L. van Wüllen, T. F. Fässler, *Chem. Mater.* **2018**, *30*, 6440–6448.

[23] H. Eickhoff, C. Sedlmeier, W. Klein, G. Raudaschl-Sieber, H. A. Gasteiger, T. F. Fässler, *Z. Anorg. Allg. Chem.* **2020**, *646*, 95–102.

[24] A. Haffner, V. Weippert, D. Johrendt, *Z. Anorg. Allg. Chem.* **2020**, zaac.202000296.

[25] H. G. von Schnering, G. Menge, *Journal of Solid State Chemistry* **1979**, *28*, 13–19.

[26] J. Mark, J. Wang, K. Wu, J. G. Lo, S. Lee, K. Kovnir, *J. Am. Chem. Soc.* **2019**, *141*, 11976–11983.

[27] A. Haffner, D. Johrendt, *Z. Anorg. Allg. Chem.* **2017**, *643*, 1717–1720.

[28] A. Haffner, V. Weippert, D. Johrendt, *Z. Anorg. Allg. Chem.* **2020**, *646*, 120–124.

[29] J. Mark, J.-A. Dolyniuk, N. Tran, K. Kovnir, *Z. Anorg. Allg. Chem.* **2019**, *645*, 242–247.
[30] S. Strobel, T. Schleid, *Angew. Chem. Int. Ed.* **2003**, *42*, 4911–4913.
[31] P. Kaiser, W. Jeitschko, *Journal of Solid State Chemistry* **1996**, *124*, 346–352.
[32] B. Eisenmann, *Zeitschrift für Naturforschung B* **1984**, *39*, 736–738.
[33] H. Vincent, J. Kreisel, Ch. Perrier, O. Chaix-Pluchery, P. Chaudouet, R. Madar, F. Genet, G. Lucazeau, *Journal of Solid State Chemistry* **1996**, *124*, 366–373.
[34] J.-A. Dolyniuk, D. C. Kaseman, S. Sen, J. Zhao, F. E. Osterloh, K. Kovnir, *Chem. Eur. J.* **2014**, *20*, 10829–10837.
[35] J.-A. Dolyniuk, H. He, A. S. Ivanov, A. I. Boldyrev, S. Bobev, K. Kovnir, *Inorg. Chem.* **2015**, *54*, 8608–8616.
[36] R. C. Fischer, P. P. Power, *Chem. Rev.* **2010**, *110*, 3877–3923.
[37] L. Liu, D. A. Ruiz, D. Munz, G. Bertrand, *Chem* **2016**, *1*, 147–153.
[38] J. Wang, K. Lee, K. Kovnir, *Inorg. Chem.* **2015**, *54*, 890–897.
[39] J. Wang, Y. He, N. E. Mordvinova, O. I. Lebedev, K. Kovnir, *Chem* **2018**, *4*, 1465–1475.
[40] J. Wang, P. Yox, J. Voyles, K. Kovnir, *Crystal Growth & Design* **2018**, *18*, 4076–4083.
[41] J. Wang, K. Lee, K. Kovnir, *Inorg. Chem.* **2017**, *56*, 783–790.
[42] H. T. Stokes, D. M. Hatch, B. J. Campbell, *FINDSYM, ISOTROPY Software Suite*, **n.d.**
[43] H. T. Stokes, D. M. Hatch, *J Appl Crystallogr* **2005**, *38*, 237–238.
[44] G. M. Sheldrick, *Acta Crystallogr A Found Crystallogr* **2008**, *64*, 112–122.
[45] G. Kresse, J. Furthmüller, *Phys. Rev. B* **1996**, *54*, 11169–11186.
[46] G. Kresse, D. Joubert, *Phys. Rev. B* **1999**, *59*, 1758–1775.
[47] P. E. Blöchl, *Phys. Rev. B* **1994**, *50*, 17953–17979.
[48] J. P. Perdew, K. Burke, M. Ernzerhof, *PHYSICAL REVIEW LETTERS* **1996**, *77*, 4.
[49] J. P. Perdew, *Int. J. Quantum Chem.* **1985**, *28*, 497–523.
[50] P. E. Blöchl, O. Jepsen, O. K. Andersen, *Phys. Rev. B* **1994**, *49*, 16223–16233.
[51] H. J. Monkhorst, J. D. Pack, *Phys. Rev. B* **1976**, *13*, 5188–5192.

10.1002/zaac.202000378

# For Table of Contents Figure Only

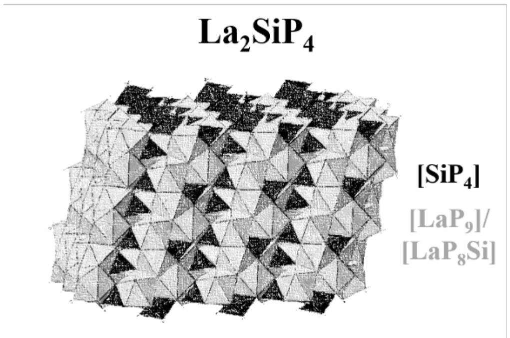

Artistic rendition of the structure of $La_2SiP_4$ as a polyhedral model, showing $SiP_4$ and $LaP_9$/$LaSiP_8$ units.